



Deep-Seated Slope Stability Analysis and Development of Simplistic FOS Evaluation Models for Stone Column-Supported Embankments

Lateef Ahmad Dar¹  · Mohammad Yousuf Shah¹

Accepted: 30 July 2020 / Published online: 5 August 2020
© Springer Science+Business Media, LLC, part of Springer Nature 2020

Abstract

Inclusion of stone columns in the underlain soft soil is one of the most prominent methods for improving the stability of embankments. The stone columns are encased with a geosynthetic material to further enhance the stability. The influence of this partial replacement of weak foundation soil with stone columns on the performance of embankments needs to be quantified. In this study, performance of ordinary stone column (OSC) and geosynthetic-encased stone column (GESC)-supported embankments is carried out using a three-dimensional finite element programme (PLAXIS3D). A parametric study was conducted to quantify the influence of various factors viz. spacing to diameter ratio (S/D), stiffness of encasement, cohesion of soil, friction angle of stone column and friction angle of embankment on the factor of safety against deep-seated failure. The results show that encasing the stone columns enhances the stability of embankments. Decreasing the column spacing (S/D) enhances the stability, reduces the excess pore pressure development and average settlement. Increase in geotextile encasement stiffness, cohesion of underlain soft soil, friction angle of stone column and friction angle of embankment improves the performance of embankments and also reduces the average settlement of the ground under embankment. Results of the parametric study were used to develop two types of data-driven models viz. multiple linear regression (MLR) and artificial neural networks (ANN) to simplify the evaluation of the factor of safety (FOS) of embankments. Among the two approaches, ANNs were able to predict the factor of safety values more accurately.

Keywords Deep-seated failure · Geotextile encasement · Finite element method · MLR · ANN

✉ Lateef Ahmad Dar
lateefdar_10phd18@nitsri.net; lateefahmad90@gmail.com

Mohammad Yousuf Shah
yousuf@nitsri.net

Extended author information available on the last page of the article

1 Introduction

The instability of embankments founded on soft soils presents huge problems to geotechnical engineers. The various types of slope instability issues comprise of local, surficial, general and deep-seated slope failures respectively. When the underlain foundation soil is weak, deep-seated slope failure is more predominant in those situations. This becomes a huge issue while constructing road embankments on soft soils. Figure 1 shows the various types of potential slope failures that can occur in embankments. Various methods have been developed over the years to address this issue; these include reinforcing the underlain soft soil with sand compaction piles, deep-mixed columns and stone columns etc. Among these methods, reinforcing the foundation soil by inclusion of stone columns has been effectively used to solve the issue of deep-seated slope instability and is effective in flexible loading conditions like oil storage tanks and embankments (Hughes et al. 1975; McKenna et al. 1975; Aboshi et al. 1979; Bergado et al. 1990; Cooper and Rose 1999; Zhang et al. 2014). The effectiveness of stone columns is dependent upon the amount of lateral confinement provided by the neighbouring soil. Under very soft soil conditions, the surrounding soil is not able to provide adequate passive resistance, thereby reducing the load-carrying capacity of the stone column. To overcome this issue, the stone columns are suitably encased by geosynthetic material in such situations to overcome the deficiency in the passive resistance offered by the surrounding soil. The encasement provides additional stiffness to the stone column by mobilisation of hoop stress in the reinforcing material (Van and Silence 1986; Murugesan and Rajagopal 2006; Malarvizhi and Ilamparuthi 2007; Ghazavi and Afshar 2013). The encasement material has high axial stiffness; large stresses are needed to be mobilised in the encasement material to undergo any considerable strain. Hence, the geosynthetic encasement simulates stiff soil conditions. The effect of encasement on the performance of stone column is well documented (Murugesan and Rajagopal 2006; Raithel and Kempfert 2000; Sharma et al. 2004;

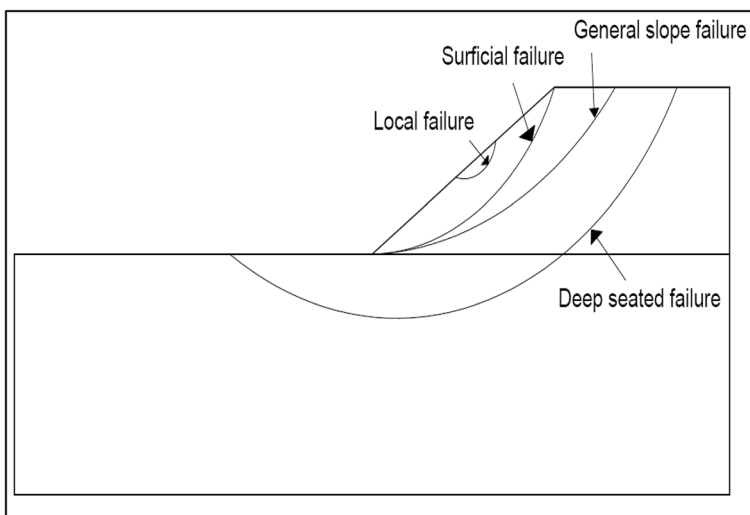


Fig. 1 Potential slope stability failures (Han et al., 2004)

Ayadat and Hanna 2005; Brokemper et al. 2006; Yoo et al. 2007; Murugesan and Rajagopal 2007; Gniel and Bouazza 2009; Wu and Hong 2009; Ali et al. 2012, Yoo and Lee 2012, Murtaza and Samadhiya 2016). The stability of stone columns in the foundation soil directly influences the stability of overlying embankments. When embankments are built on stone column-reinforced foundations, the columns under the embankments experience an amalgam of stresses in various directions and may fail in shearing, bending, sliding, tension, rotation or a combination of various failure modes (Kivelo and Broms 1999; Han et al. 2005; Kitazume and Maruyama 2006; Han 2012; Zhan Zheng et al., 2014). Under soft soil conditions, the vertical and lateral stability of ordinary stone columns is not enough to resist the deep-seated failure. To overcome this issue, the stone columns may be encased with a geosynthetic material of very high axial stiffness. Providing stone columns in foundation soil not only enhances the stability but also helps in increasing the rate of consolidation as the stone column infill has very high permeability compared with the soft soil (Greenwood 1970; Priebe 1995; Han and Ye 2001; Castro et al. 2013) and can also be used as an effective liquefaction countermeasure (Adalier and Elgamal 2004). The geosynthetic encasement gives 2-fold advantage as it confines the infill material, and also, it acts as a barrier between the infill and surrounding soil. The encasement material can be of various types viz. geotextiles, geogrids etc. The axial stiffness of these materials is very large and huge hoop stresses need to be mobilised to undergo any considerable lateral strain. Various numerical studies have been conducted in the past to analyse the behaviour of embankments supported by stone column-reinforced ground (Yoo and Kim 2009; Lo et al. 2010; Yoo 2010; Abusharar and Han 2011; Tandel et al. 2013; Khabbazian et al. 2014; Zhang Z et al., 2014; Khadim and Fouad 2018). Due to complexity of three-dimensional models, most of the researches on deep-seated slope stability have been carried out using two-dimensional numerical approaches as three-dimensional numerical methods are complex and need special computational resources. The three-dimensional numerical analysis is more realistic and accurate.

This study uses a three-dimensional FE programme PLAXIS3D to analyse the influence of reinforcing the weak foundation soil with OSCs and GSCs on stability of embankments against the deep-seated failure. Three-dimensional numerical analysis is a better representation of any physical process because it takes into account the variability of the system in the third dimension also. Hence, three-dimensional numerical analyses give more reliable results. In this study, the unreinforced embankment was first analysed; then, the influence of reinforcing the soft soil with OSC and GESC on the stability of the embankment was quantified. The effect of various factors on the stability of embankments was analysed. The influence of variation in S/D ratio, geosynthetic encasement stiffness (J), cohesion of foundation soil, friction angle of stone column infill and friction angle of embankment fill on the performance of embankments was analysed and quantified. After conducting the parametric study, two types of data-driven models viz., multiple linear regression (MLR) and artificial neural networks (ANN), were developed to simplify the prediction of factor of safety (FOS) of embankments against the deep-seated failure. MLR and ANNs have the ability to generate interrelationships between the output and the influencing variables, and these interrelationships can then be used for prediction of outputs for any set of input variables. This ability makes them useful for various complex geotechnical engineering problems. In this study, the feasibility of using MLR and ANN for

prediction of FOS against the deep-seated failure is analysed. The data of the parametric study was used for development of these models, and the reliability of the models to predict the FOS was analysed by testing the models on 15 independent model outputs that were not used during the developmental stage of the models.

2 Finite Element Analysis

The investigation in this study was carried out using a commercial FE programme, PLAXIS3D. This FE package provides an environment for solving complex geotechnical engineering problems in which the soil behaviour is simulated by development of 3D soil models. This FEM package comprises of robust computational procedures that have been well tested over the years. The behaviour of embankments on OSC and GESC reinforced ground was analysed by development of 3D embankment models.

2.1 Model Geometry

The cross section of embankment used in this study is shown in Fig. 2. The embankment is 40 m wide, 5 m high with side slope of 1:2. The embankment is constructed on soft soil of 10 m thickness. The bottom layer comprises of dense sand layer of 2 m thickness. Columns of 0.5 m diameter and 10 m length were taken for this study. For the benchmark case, the S/D ratio was taken as 3 which corresponds to spacing of 1.5 m between the columns. As the embankment is symmetrical along the central vertical axis, only half of the embankment was taken up for analysis. The embankment geometry, spacing and dimensions of columns were assumed based on the common practices in the field. Same model geometry has been used by various researchers in the past (Han et al. 2007; Abusharar and Han 2011; Zhang et al. 2014).

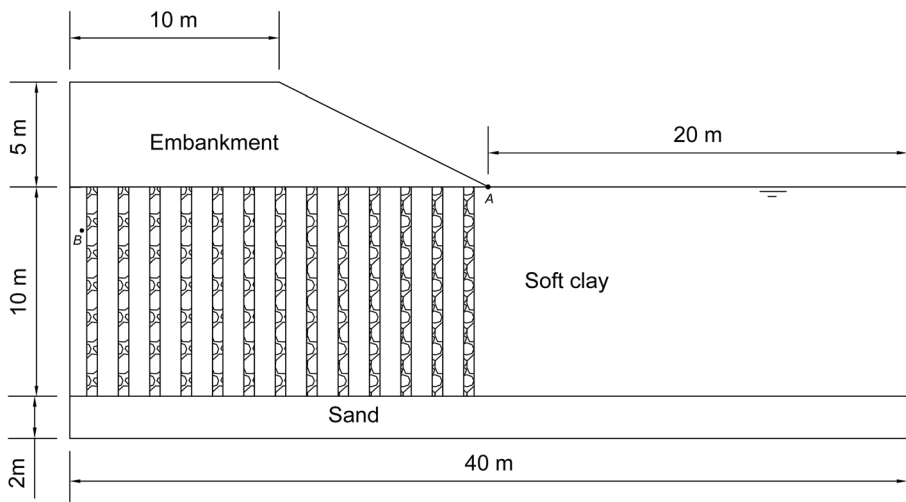


Fig. 2 Model geometry

2.2 Material Modelling and Parameters

The embankment, soft soil, sand and stone columns were modelled as linearly elastic perfectly plastic materials based on Mohr-Columb failure criteria. Ten-node tetrahedral elements were used for the development of finite element meshes for these materials. The geosynthetic encasement was modelled a linearly elastic material having axial stiffness only by using a geogrid element available with PLAXIS3D. Finer mesh arrangements were used in this analysis to achieve greater accuracy.

For the benchmark case, the material parameters used in this analysis are shown in Table 1. These parameters were varied to quantify their influence on the deep-seated slope stability. The various types of models developed are shown in Fig. 3.

2.3 Safety Analysis

Excess pore water pressure development is a major concern as it results in the reduction of effective stress in the soil. Hence, the embankments are constructed in phases to allow for dissipation of excess pore water pressure. With the reduction in excess pore pressure, the soils regain its shear strength. In this study, the embankment was simulated to be constructed in stages, wherein the embankment is constructed in 5 layers of 1 m thickness each. Each layer is constructed in 10 days followed by consolidation period of 30 days. During the last consolidation phase, the calculation is continued until minimum excel pore pressure (1 kPa) condition is reached. The development of excess pore water in the underlain soft soil during the staged construction was analysed by mapping the excess pore water pressure fluctuations with time at point B (0.5, 0, - 2) as shown in Fig. 2. The FOS against the deep-seated failure is calculated at the end of construction by plotting a total multiplier $\sum Msf$ against the displacement at the node A (20, 0, 0) near the toe of embankment as shown in Fig. 2.

3 Validation of Finite Element Model

Numerical analysis of embankment stability carried out by Zhang et al. (2014) was used to validate the finite element approach used in this study. They studied the short-

Table 1 Material properties of soil and stone aggregates for benchmark case

Parameters	Soft clay	Sand	Stone column	Embankment	Geosynthetic encasement
Unsaturated unit weight (kN/m ³)	16	17	17	18	–
Saturated unit weight (kN/m ³)	19	19.5	20	20	–
Young's modulus, E (kPa)	2000	50,000	35,000	35,000	–
Poisson's ratio	0.40	0.3	0.30	0.35	–
Cohesion (kPa)	5	0	0	2	–
Angle of internal friction/ (ϕ°)	10	30	38	30	–
Dilatancy (ψ°)	0	0	5	0	–
Permeability, K (m/day)	5.4×10^{-5}	5.25	11.23	3.25	–
Axial stiffness, J (kN/m)	–	–	–	–	1000

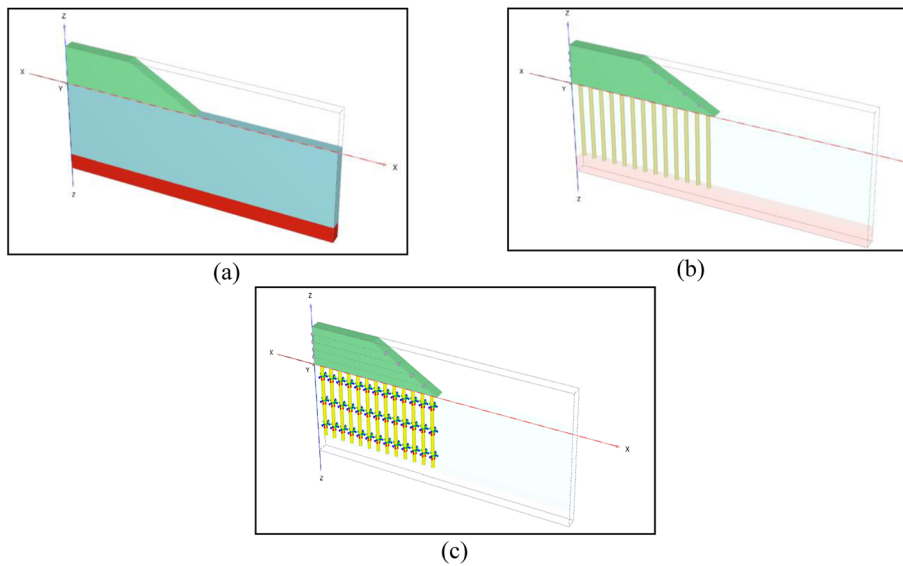
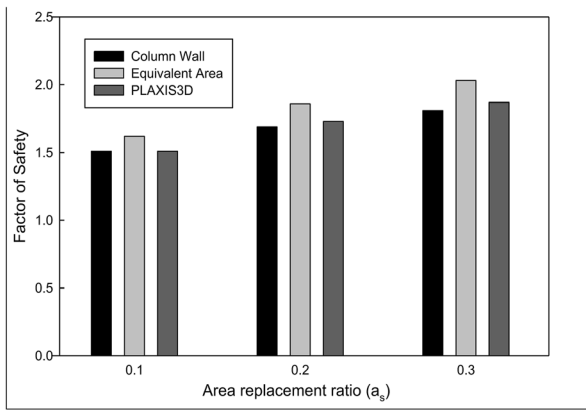


Fig. 3 a Unreinforced, b ordinary reinforced and c geosynthetic-encased stone column embankments

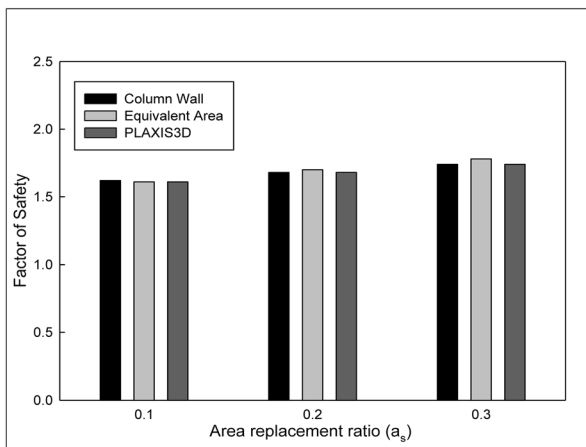
term (ST) and the long-term (LT) behaviour of stone column-supported embankments using a two-dimensional finite difference method (FLAC2D 5.0). Two-dimensional numerical modelling was carried out using two methods viz. column wall and equivalent area methods. These methods convert a three-dimensional problem into an equivalent two-dimensional plain strain condition. The shape of the embankment is similar as used in this study. A 0.45-m surface layer at the slope was assigned to prevent any surficial failure. Stone columns of 0.5 m diameter were used to reinforce the underlying ground at a spacing of 1.4 m, 1.0 m and 0.8 m that correspond to area replacement ratios (a_s) of 0.1, 0.2 and 0.3 respectively. Details of material properties as used by Zhang et al. (2014) are given in Table 2. Three-dimensional numerical models using PLAXIS3D were developed for the validation for both the short-term and long-term condition. Figure 4a shows the histogram of FOS values computed from the FLAC2D and PLAXIS3D numerical methods under short-term conditions, and Fig. 4b shows the histogram of FOS values under long-term conditions. A close agreement is observed between FOS values computed by the two numerical methods in short-term and long-term conditions. Hence, the numerical models developed using PLAXIS3D can be used to analyse the stability of column-supported embankments.

Table 2 Material properties used for validation (after Zhang et al. (2014))

Material	Diameter (m)	γ (kN/m ³)	E (MPa)	Poisson's ratio	Cohesion (kPa)	Friction angle (ϕ°)
Embankment	–	18	30	0.3	10	32
Surface	–	18	30	0.3	15	32
Clay _{ST}	–	16	4	0.45	20	0
Clay _{LT}	–	16	4	0.45	0	20
Sand	–	18	100	0.3	0	30
Stone column	0.5	17	40	0.3	0	38



(a)



(b)

Fig. 4 Histogram showing comparison of FOS values. **a** Short-term condition. **b** Long-term condition

4 Results of Parametric Studies and Discussions

Three-dimensional FE analysis using PLAXIS3D was used to analyse the influence of reinforcing the foundation soil with OSCs and GSCs on the stability of embankments. The models were first developed for the benchmark case, and then, parametric study was conducted. These parameters include the S/D ratio, geosynthetic encasement stiffness, cohesion of foundation soil, friction angle of stone column infill and friction angle of embankment fill.

4.1 Effect of S/D Ratio

The impact of spacing to diameter (S/D) ratio on the FOS, settlement and pore water pressure development was studied by analysing the embankment for varying S/D ratios of columns. The analysis was carried out for both OSC- and GESC-supported embankments. Stiffness of geosynthetic encasement, $J = 1000 \text{ kN/m}$, was taken in the

case of GESCs. The S/D ratio of the stone columns was varied as 2.0, 2.5, 3.0 and 3.5. The width of embankment was taken equal to the diameter of corresponding unit cell for triangular arrangement i.e. $1.05 \times S$ where ‘S’ is the spacing between the stone columns. It is evident from Fig. 5 that S/D ratio has considerable effect on the FOS against the deep-seated slope failure. A perusal of Fig. 5 shows as the S/D between the columns increases, there is reduction in the FOS both in OSC– and GESC–supported embankments.

Higher FOS values can be observed in the GESC–supported embankments. Higher FOS was observed at lower S/D ratios which means that larger area replacement ratios yield better FOS. The improvement in the FOS is more prominent when geosynthetic encasements are used. Increase in the S/D ratio from 2 to 3.5 lead to reduction in the FOS from 1.25 to 1.1 and 1.75 to 1.58 for OSC– and GESC–supported embankments respectively.

Excess pore water pressure development may result in embankment failures (Briggs et al. 2017). Hence, analysing the impact of reinforcing the soil with stone columns on excess pore pressure development becomes very important. The effect of partial replacement of foundation soil with the stone aggregate infill on the pore water pressure development was studied by taking the pore pressure readings with respect to time at point B as shown in Fig. 2. Variation in excess pore pressure development with varying S/D ratio at point B is shown in Fig. 6. The excess pore water pressure development is maximum for S/D = 3 and as the S/D ratio reduces, the magnitude of excess pore water pressure also reduces. It can be deduced that the stone column infill material helps in dissipation of the excess pore water pressure owing to the higher permeability of stone column infill. As the spacing between the stone columns is reduced, the area replacement ratio increases, thereby resulting in development of lesser excess pore water pressures.

The enhancement in the settlement behaviour of the embankments is expressed in terms of a factor called the settlement reduction ratio (β). It can be defined as the ratio of average settlement in the natural ground level under embankment after reinforcing the soil to the average settlement in the unreinforced ground. Lower values of ‘ β ’ mean the occurrence of lesser settlements in the ground under embankment after reinforcing.

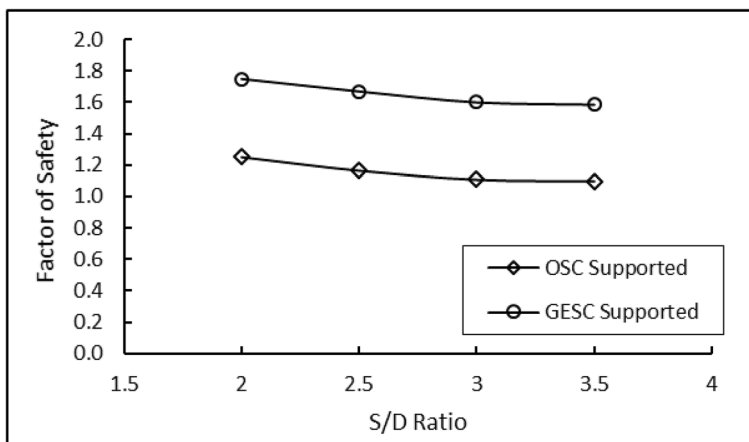


Fig. 5 Effect of S/D on the factor of safety in OSC– and GESC–supported embankments

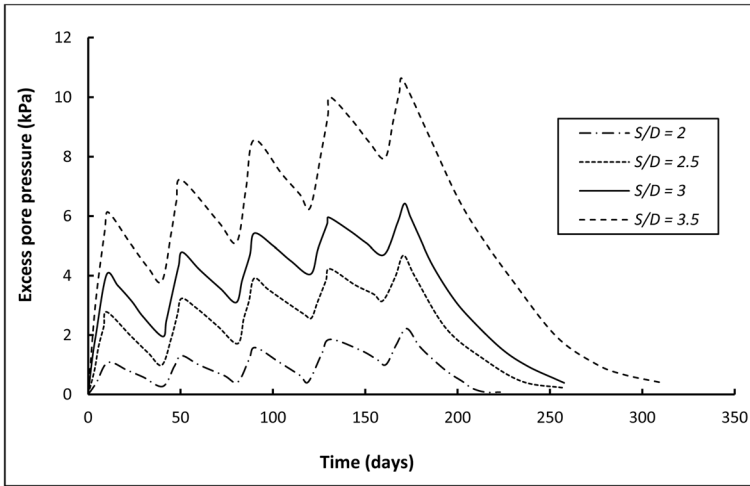


Fig. 6 Effect of S/D on the excess pore water pressure development

The influence of reinforcing the weak foundation soil by OSCs and GESCs on the settlement behaviour of the natural ground is shown in Fig. 7. As the S/D ratio reduces from 3.5 to 2, there is reduction in average settlement by 45.50% and 43.20% in the case of OSC- and GESC-supported embankments respectively.

4.2 Effect of Stiffness of Geosynthetic Encasement

Geosynthetic encasement stiffens the stone columns by providing added lateral confinement. The influence of stiffness of encasement on the stability of embankments needs to be quantified. GESC-supported embankment with columns of diameter 0.5 m and S/D = 3.0 were taken for analysis. The impact of stiffness of geosynthetic encasement on the response of embankments was analysed by varying the geosynthetic encasement stiffness as $J = 500$ kN/m, 1000 kN/m, 2000 kN/m, 3000 kN/m and 4000 kN/m. The influence of this variation of geosynthetic encasement stiffness on FOS is shown in Fig. 8. There is considerable improvement in the FOS with increasing axial stiffness of the encasement. As the geosynthetic encasement stiffness increased

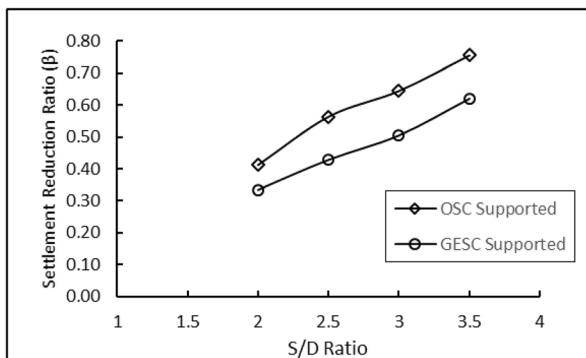


Fig. 7 Effect of S/D on the settlement reduction ratio (β)

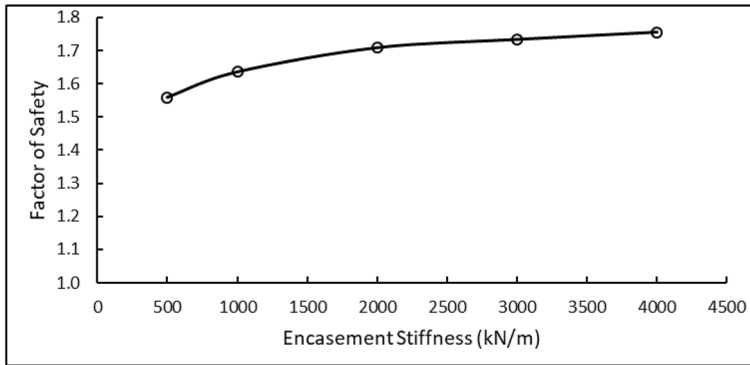


Fig. 8 Effect of geosynthetic encasement stiffness on the factor of safety

from 500 to 4000 kN/m, the FOS enhanced from 1.56 to 1.76. The improvement is more prominent at when the stiffness is increased upto 2000 kN/m beyond which, there is marginal enhancement in the factor of safety.

The variation in the development of excess pore water pressure on increasing geosynthetic encasement stiffness is shown in Fig. 9. With increase in the stiffness of encasement, the magnitude of excess pore water pressure reduces. It can be attributed to the fact that higher encasement stiffness makes the columns stiffer, as a result of which larger embankment loads are borne by the GESC's and there is reduced embankment load on the soft clay.

The impact of increasing stiffness of encasement on the settlement of the natural ground is expressed in terms of average settlement under the embankment as shown in Fig. 10. The average settlement under the embankment reduced from 0.638 to 0.562 m which corresponds to the reduction of 11.91% in the average settlement under the embankment on increasing the axial stiffness of the encasement from 500 to 4000 kN/m.

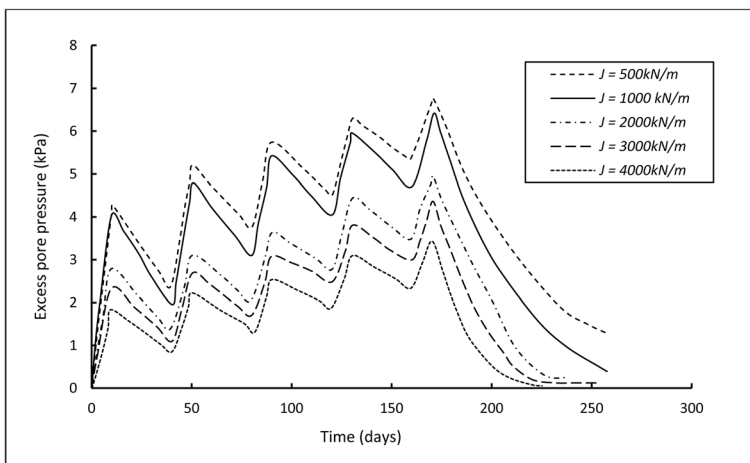


Fig. 9 Development of excess pore water pressure with time for varying encasement stiffness (J)

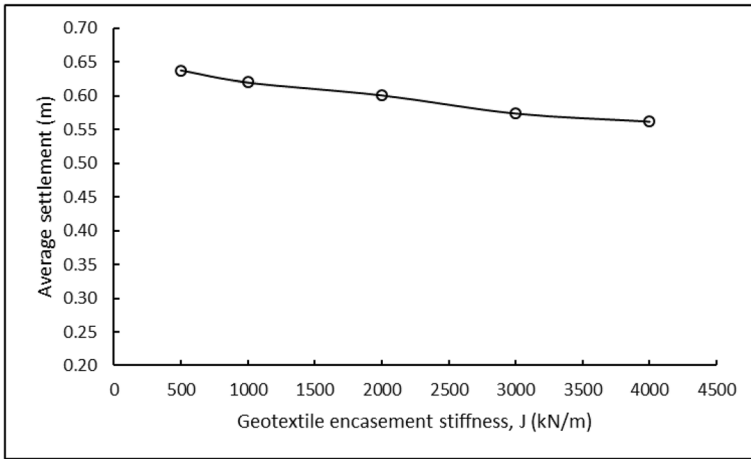


Fig. 10 Variation in average settlement on increasing the geosynthetic encasement stiffness

4.3 Effect of Cohesion of Soft Soil

The nature and extent of failure in an embankment depends upon the strength of underlain soil. To study the effect of cohesion of the foundation soil on the stability of the embankments, the cohesion of the soft soil was varied as 5 kPa, 10 kPa, 20 kPa, 30 kPa and 40 kPa. The improvement in the FOS with varying cohesion was analysed for unreinforced, OSC–reinforced and GESC–reinforced foundation soil conditions. The impact of varying cohesion of underlain soft soil on the stability of the embankment is shown in Fig. 11. The FOS improves considerably with increasing cohesion. The GESC–supported embankments showed higher FOS. On increasing the cohesion from 5 to 40 kPa, the FOS improved from 1.02 to 1.61, 1.11 to 1.69 and 1.64 to 1.9 for unreinforced, OSC–supported and GESC–supported embankments. The improvement was more prominent for smaller values of cohesion. On increasing the cohesion above 20 kPa, there is marginal improvement in the FOS. At larger values of cohesion, the

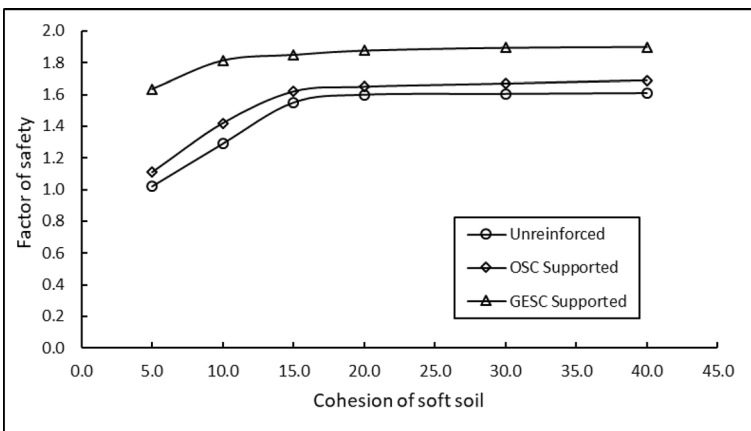


Fig. 11 Effect of cohesion of soil on the factor of safety

failure pattern changes and the failure occurs above the foundation soil as shown in Fig. 12.

The impact of cohesion of underlain soil on the average settlement under the embankment is shown in Fig. 13. The settlement reduction ratios for GESC-supported embankments are lower than OSC-supported embankments which means that former undergo smaller settlements. On increasing the cohesion from 5 to 40 kPa, the settlement reduction ratio (β) reduces by 15.83% and 18.81% for OSC- and GESC-supported embankments respectively.

4.4 Effect of Friction Angle of Stone Column

To analyse the influence of friction angle of the stone column infill material on the behaviour of embankment, the friction angle of the stone column was varied as 30°, 34°, 38° and 42° keeping all other parameters as constant. The influence of frictional angle of stone columns on the FOS is shown in Fig. 14. The FOS increases with increasing friction angle of stone column for both OSC- and GESC-supported embankments which means that better quality aggregates yield higher FOS values. On varying the friction angle of the stone column infill from 30° to 42°, the FOS values increased from 1.08 to 1.13 and 1.58 to 1.67 for OSC- and GESC-supported embankments respectively.

With increase in the friction angle of stone column, the settlement reduction ratio reduces as shown in Fig. 15. The settlement reduction ratio reduces by 15.33% and 14.44% for OSC- and GESC-supported embankments respectively on increasing the frictional angle from 30°–42°.

4.5 Effect of Friction Angle of Embankment

The influence of quality of embankment fill material on the stability of embankment was analysed by varying the friction angle of embankment as 25°, 30°, 35° and 40°.

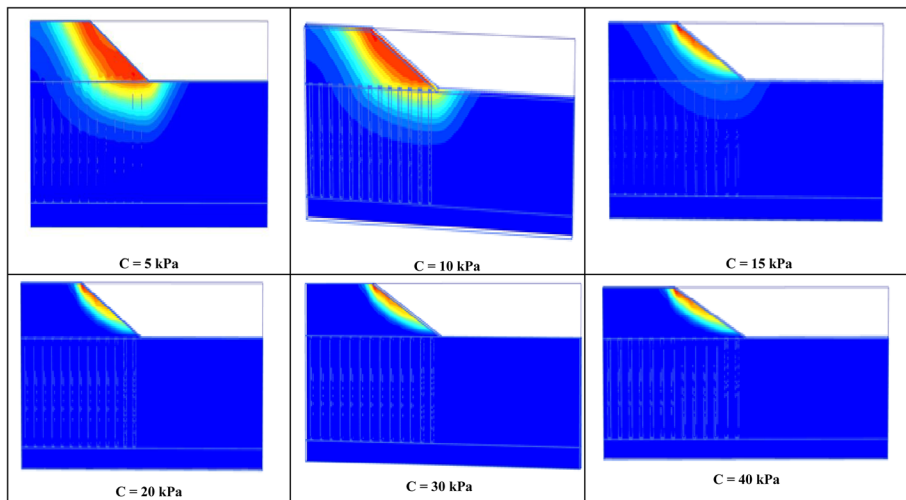


Fig. 12 Progression of mode of failure for various values of cohesion of foundation soil

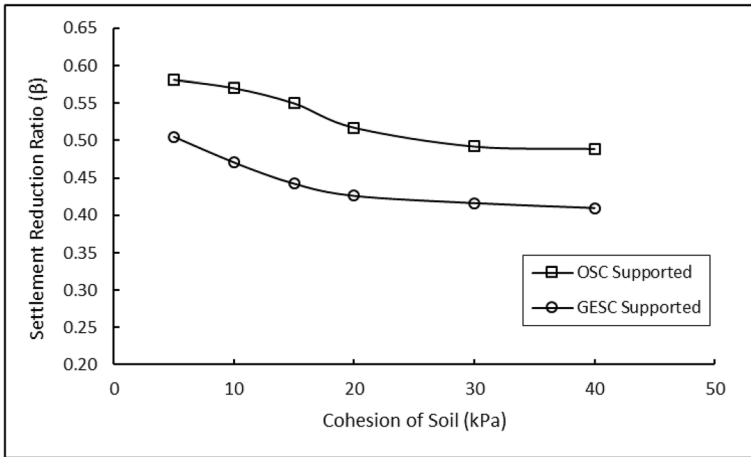


Fig. 13 Effect of cohesion of foundation soil on the settlement reduction ratio (β)

Figure 16 shows the impact of friction angle of embankment on the FOS of unreinforced, OSC– and GESC–supported embankments. On increasing the friction angle of embankments from 25° to 40°, the FOS improved from 1.01 to 1.09, 1.07 to 1.18 and 1.50 to 1.87 for unreinforced, OSC supported and GESC–supported embankments. There is mild improvement in the FOS values in unreinforced and OSC–supported embankments, but in the case of GESC–supported embankments, the improvement is more prominent.

The impact of friction angle of embankment fill on the settlement reduction ratio is shown in Fig. 17. The settlement reduction ratio (β) decreased on increasing the frictional angle of embankment from 25° to 40°. The settlement reduction ratio reduced by 4.5% and 5.21% for OSC– and GESC–supported embankments respectively. Hence, better quality embankments undergo smaller settlements.

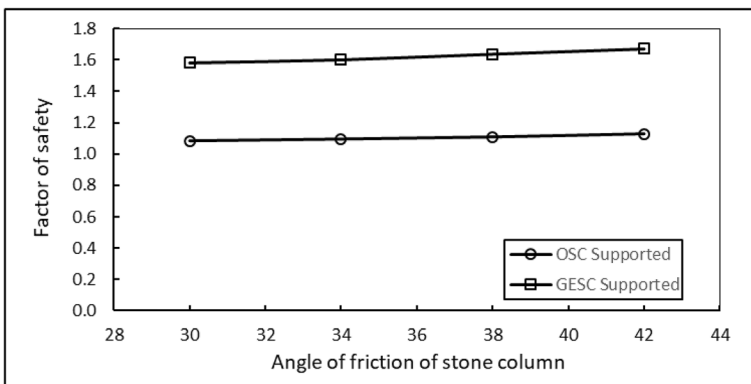


Fig. 14 Effect of friction angle of stone columns on the factor of safety

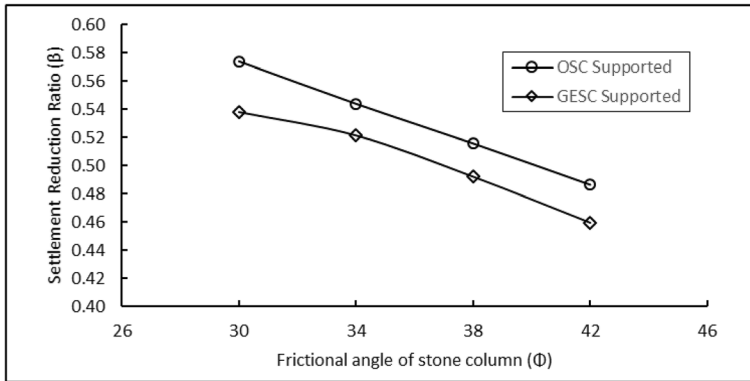


Fig. 15 Effect of frictional angle of stone column on the settlement reduction ratio (β)

5 Development of Simplistic FOS Evaluation Models

Since the numerical analysis of ordinary and encased stone column-supported embankments is a very complex process and it may not always be possible to have the required computational resources, simple and accurate methods for evaluation of stability of such embankments are needed. Hence, two simplistic data-driven models viz. multiple linear regression (MLR) and artificial neural networks (ANN) were developed to simplify the evaluation of factor of safety of stone column-supported embankments. The data generated from the parametric study was used for the development of these models. A total of 51 embankments were analysed during the parametric study, and the data generated as shown in Table 3 was used to develop the models. Table 3 shows variation in FOS values for corresponding variation in various influencing parameters viz. cohesion of soft soil (C), friction angle of stone column infill (ϕ_{sc}), friction angle of embankment fill (ϕ_{emb}), spacing to diameter ratio (S/D) and geotextile encasement stiffness (J).

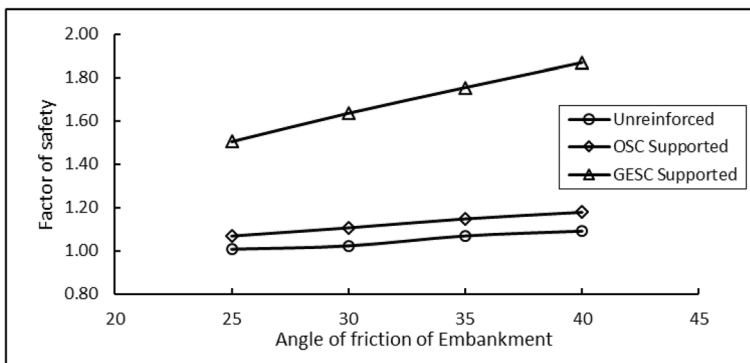


Fig. 16 Effect of friction angle of embankment on factor of safety

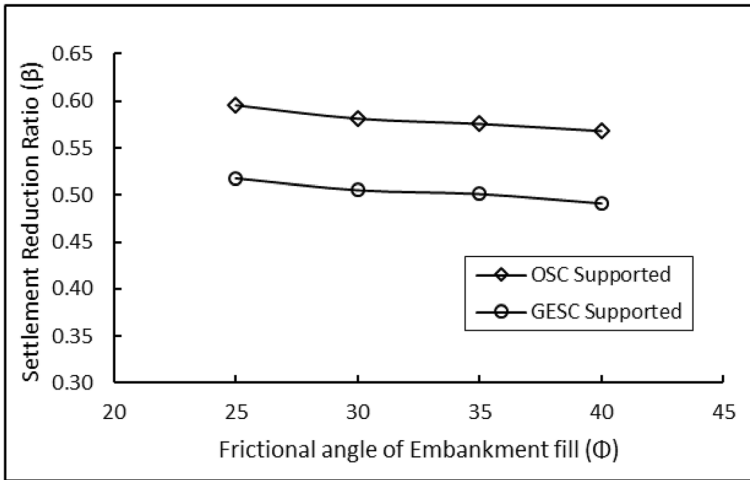


Fig. 17 Effect of friction angle of embankment on the settlement reduction ratio (β)

5.1 Development of Multiple Linear Regression Model

Multiple linear regression is a mathematical tool for developing relationships between the outputs and influencing variables. In this study, the relationship between the FOS against the deep-seated failure and the various soil parameters was modelled using a multiple linear regression technique. Multiple linear regression (MLR) tries to fit a polynomial equation between the input and output variables. The general structure of the MLR model is as:

$$y = a_0 + a_1x_1 + \dots + a_nx_n + \varepsilon$$

where

- y output/response/dependent variable
- x_1, x_2, x_n input/independent/predictor
- a_0, a_1, a_n regression coefficients
- a_0 constant
- and ε error.

The value of regression coefficient determines the contribution of an independent variable on the output. MLR is aimed at predicting the values of these regression coefficients to arrive at the best fit linear polynomial curve. This regression line represents the relationship between the input and output variables. This regression equation can be used to determine the output values for any set of independent variables. Generally, the regression line is not a perfect fit that means it may not exactly fit all the data points. The goodness of fit of the regression line is represented in terms of coefficient of determination (R^2) which is expressed as

Table 3 Data used for development of MLR and ANN

S. no	Factor of safety	Cohesion of clay C (kPa)	Friction angle of stone column (ϕ_{sc})	Friction angle of embankment (ϕ_{emb})	S/D ratio	Geosynthetic encasement stiffness J (kN/m)
1	1.02	5	0	30	0	0
2	1.29	10	0	30	0	0
3	1.55	15	0	30	0	0
4	1.65	20	0	30	0	0
5	1.64	30	0	30	0	0
6	1.71	40	0	30	0	0
7	1.00	5	0	25	0	0
8	1.02	5	0	30	0	0
9	1.07	5	0	35	0	0
10	1.09	5	0	40	0	0
11	1.25	5	38	30	2	0
12	1.16	5	38	30	2.5	0
13	1.11	5	38	30	3	0
14	1.1	5	38	30	3.5	0
15	1.75	5	38	30	2	1000
16	1.67	5	38	30	2.5	1000
17	1.60	5	38	30	3	1000
18	1.58	5	38	30	3.5	1000
19	1.56	5	38	30	3	500
20	1.64	5	38	30	3	1000
21	1.71	5	38	30	3	2000
22	1.73	5	38	30	3	3000
23	1.76	5	38	30	3	4000
24	1.11	5	38	30	3	0
25	1.42	10	38	30	3	0
26	1.62	15	38	30	3	0
27	1.65	20	38	30	3	0
28	1.67	30	38	30	3	0
29	1.69	40	38	30	3	0
30	1.64	5	38	30	3	1000
31	1.81	10	38	30	3	1000
32	1.85	15	38	30	3	1000
33	1.88	20	38	30	3	1000
34	1.90	30	38	30	3	1000
35	1.92	40	38	30	3	1000
36	1.08	5	30	30	3	0
37	1.10	5	34	30	3	0
38	1.11	5	38	30	3	0
39	1.13	5	42	30	3	0
40	1.58	5	30	30	3	1000

Table 3 (continued)

S. no	Factor of safety	Cohesion of clay C (kPa)	Friction angle of stone column (ϕ_{sc})	Friction angle of embankment (ϕ_{emb})	S/D ratio	Geosynthetic encasement stiffness J (kN/m)
41	1.60	5	34	30	3	1000
42	1.64	5	38	30	3	1000
43	1.67	5	40	30	3	1000
44	1.07	5	38	25	3	1000
45	1.11	5	38	30	3	1000
46	1.15	5	38	35	3	1000
47	1.18	5	38	40	3	1000
48	1.50	5	38	25	3	1000
49	1.64	5	38	30	3	1000
50	1.76	5	38	35	3	1000
51	1.87	5	38	40	3	1000

$$R^2 = 1 - \frac{\text{Total Variation}}{\text{Explained Variation}}$$

which may also be expressed as

$$R^2 = 1 - \frac{\sum_{i=1}^n (y_p - y_a)^2}{\sum_{i=1}^n (y_a - y_m)^2}$$

where,

- n no. of observations
- y_p output or predicted value obtained from the model
- y_a actual value
- y_m average of actual values

The value of R^2 determines the strength between the variables; the value of R^2 varies between 0 and 1. It explains the variability of the response data around the mean. The value of R^2 should be close to 1 for better fit.

Data from the parametric study was used to develop MLR models. In this study, multiple linear regression analysis was carried out between the FOS and influencing parameters viz. cohesion of soft soil (C), friction angle of stone column infill (ϕ_{sc}), friction angle of embankment fill (ϕ_{emb}), spacing to diameter ratio (S/D) and geotextile encasement stiffness (J). To generalise the MLR equation, a parameter ‘ T ’ was introduced for labelling the unreinforced, OSC supported and GESC-supported embankments with values of 0, 1 and 2 respectively. The regression output for the developed MLR is shown in Table 4. The value of R^2 is 0.86 which means a very good fit between the FOS and input variables.

Table 4 Regression statistics

Parameter	Coefficients	Standard error	<i>t</i> stat	<i>P</i> value
Multiple <i>R</i>	0.930188			
<i>R</i> square	0.86525			
Adjusted <i>R</i> square	0.846875			
Standard error	0.115912			
Observations	51			
Intercept	0.767293	0.182397	4.206706	0.000125
<i>C</i>	0.017332	0.001656	10.46327	1.62E-13
ϕ_{sc}	0.000618	0.004739	0.130487	0.896776
ϕ_{emb}	0.009415	0.005634	1.671145	0.101792
S/D	-0.12816	0.057775	-2.21833	0.03174
<i>J</i>	5.75E-05	3.2E-05	1.798442	0.078969
<i>T</i>	0.390893	0.052982	7.377798	3.21E-09

5.2 Development of Neural Network Model

Artificial neural networks (ANNs) are computational models which resemble the biological neural networks present in animal brain. ANNs have the ability to learn from examples and establish relations between influencing parameters and the outputs of a complex process which makes it a very useful tool in modelling complex geotechnical engineering problems. Hence, they are also called black box models. ANNs are considered one of the most advanced data-driven techniques for solving complex problems and hence are frequently applied. Artificial neural networks have been used by various researchers for solving various complex geotechnical engineering problems in the past like prediction of bearing capacity of stone columns (Chakraborty and Goswami 2017) and prediction of slope stability (Das and Dey 2017). ANNs are composed of layers of data processing units called neurons. These neurons act as data processors and data processed in one layer is passed to another layer through connections. A typical feed forward neural network is shown in Fig. 18. These neurons convert the data into weighted sums, the weights to every input is determined while training the networks. The weight of any input represents the magnitude of influence it has on the output of any process. The weighted sums are then converted into outputs by employing a non-linear transformation function called as activation function. The layers of neurons are classified into three types i.e. an input layer, one or more hidden layers and an output layer.

The number of neurons in the input and output layer will depend upon the number of influencing parameters and the number of model outputs respectively. The determination of the number of hidden layers and the number of neurons in each layer are crucial because the network architecture is data-specific. The optimisation of the network architecture is done by trial and error method as there is no direct method of determining it. The network architecture is fixed such that the error is minimum. The neural network converts the inputs into weighted sums also expressed as:

$$\text{sum} = (X_1W_1 + X_2W_2 + \dots) + \beta \text{ where,}$$

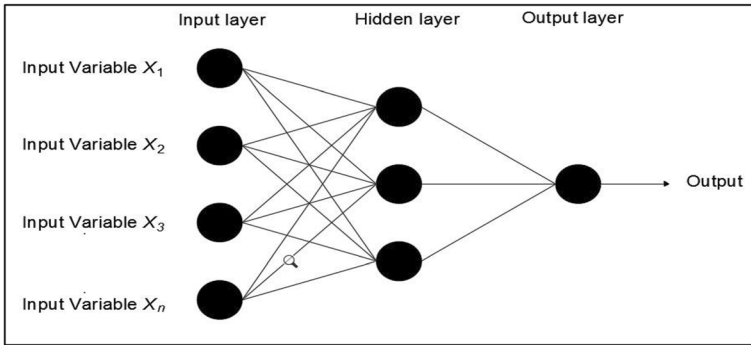


Fig. 18 Typical feed forward neural network

- X_1, X_2 inputs
- W_1, W_2 weights
- β bias

The output Y is computed as: $Y = f(\text{sum})$ where function ‘ f ’ controls the output of the network. This function is called as activation function. There are numerous types of activation functions viz. threshold, piecewise linear and sigmoidal function. Among the various activation functions, sigmoidal function is the most commonly used function (Demuth and Beale 1995). The process of assigning the weights to every input vector is called training of the network. The weights are optimised in such a way so that the error reaches a sufficiently small value. However, there is danger of over fitting a network in this fashion. To avoid this, cross validation is done on a portion of data set by dividing the input vector into three groups viz. training set, a validation set and a testing.

The data from the parametric study as shown in Table 3 was used to develop the neural network model. To generalise the ANN models, a parameter ‘ T ’ was introduced as done in case of MLR. The artificial neural network models were developed in ‘MATLAB 2018a’ workspace. In this study, a feed forward neural network with one hidden layer was used. The number of neurons in the hidden layer was determined by trial and error method. Hidden layer with 20 neurons was selected. Seventy percent of the data was used for training, 15% for validation and 15% for testing. Levenberg-Marquardt algorithm was used for training as it is the most commonly used training algorithm for feed forward neural networks. The developed neural network is shown in Fig. 19.

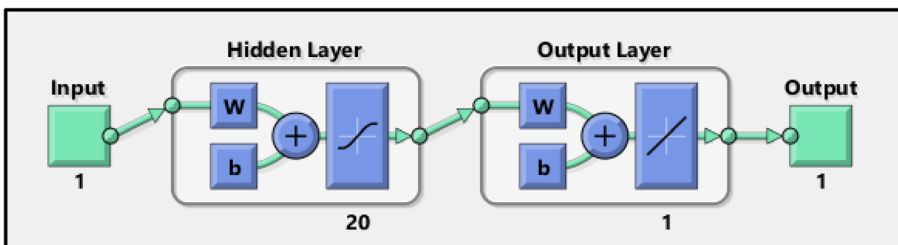


Fig. 19 View of the neural network model

The performance of neural network during training is shown in Fig. 20. The value of ‘R’ for training, validation and testing is around 0.99 which means the developed neural network can model the response of the embankment i.e. factor of safety with great accuracy.

5.3 Performance of MLR and ANN

There is lack of adequate data on three-dimensional stability analysis against deep-seated failure in literature as most of the research has been carried out using 2D numerical methods. Three-dimensional numerical models are more close to reality as they take into account the variability in the third dimension as well. Hence, the performance of the developed MLR and ANN models was checked by developing 15 FEM models in PLAXIS3D with varying parameters, and the output values of FEM were compared with the outputs of MLR and ANN. These embankments were not used during the developmental phase of MLR and ANN models. The regression plot showing the FEM vs predicted model output for MLR and ANN is shown in Fig. 21 and Fig. 22 respectively. It can be seen that the correlation coefficient for both MLR and ANN is higher than 0.9 which means that the observed and the predicted values are in close correlation. However, it can also be seen that ANN showed better correlation compared with MLR.

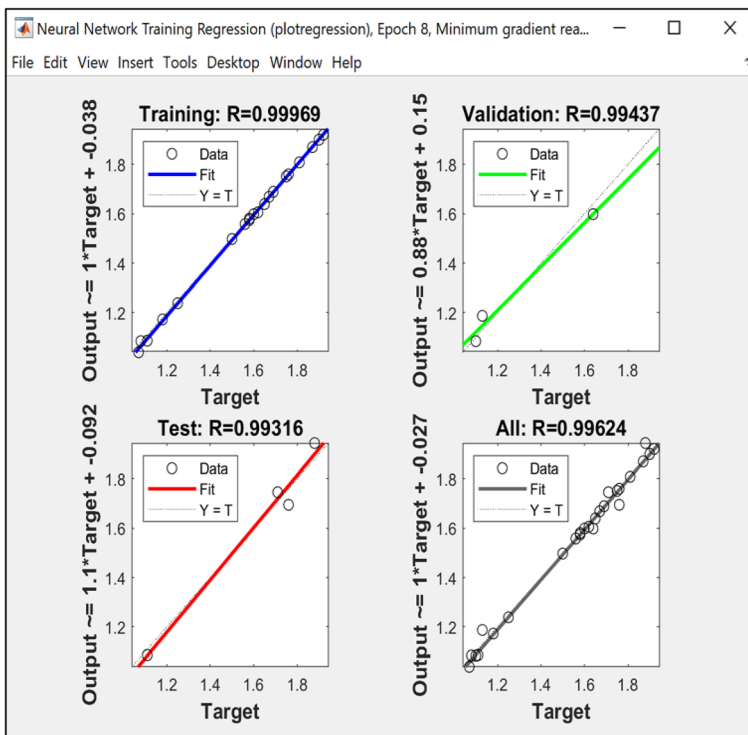


Fig. 20 Dialogue box showing performance during training, testing and cross validation

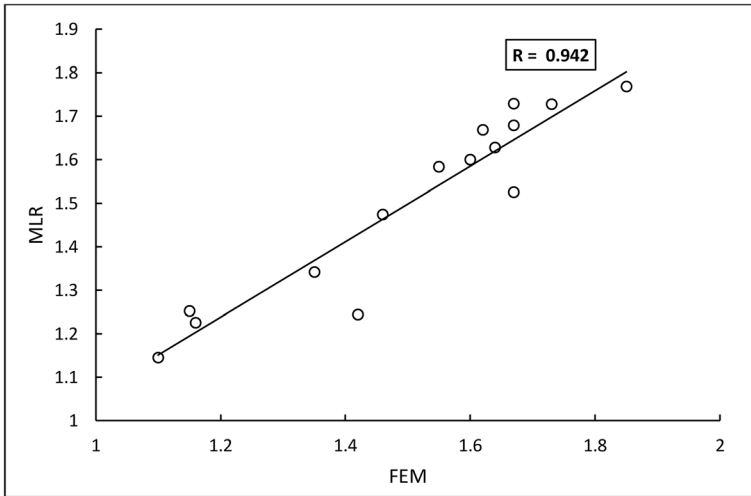


Fig. 21 Plot between predicted (MLR) and observed (FEM) values

The comparison of performance of the two models was done using three statistical parameters viz. R^2 , root mean square error (RMSE) and mean absolute error (MAE). The correlation between FEM and ANN is about 99% compared with the correlation of 94% between FEM and MLR. Hence, it can be concluded that ANN models could predict the FOS values better compared with the MLR model. This is also evident from the other statistical parameter i.e. RMSE and MAE values as shown in Table 5.

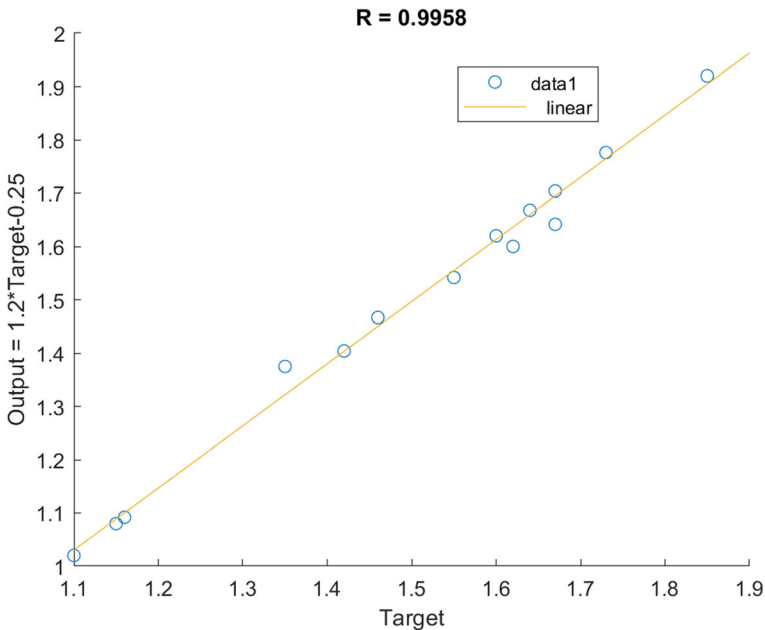


Fig. 22 Plot between predicted (ANN) and observed (FEM) values

Table 5 Comparison of various performance parameters

Model	<i>R</i>	RMSE	MAE
MLR	0.942	0.090	0.080
ANN	0.995	0.050	0.0538

6 Conclusions

Numerical analysis using a three-dimensional FE programme (PLAXIS3D) was carried out to analyse the safety of embankments against deep-seated failure. The embankments were constructed in layers of 1 m thickness and consolidation analysis followed by safety analysis was carried out. The effect of various factors on the factor of safety was analysed by conducting a parametric study. The data obtained from the parametric study was used to develop two types of data-driven models viz. MLR and ANN. These models can be used to simplify the prediction of FOS of embankments against the deep-seated failure. The reliability of these developed models was analysed by testing the models on 15 independent data sets of embankments generated from FEM. Following conclusions can be drawn from this study.

1. GESC-supported embankments exhibit higher FOS values compared with the embankments on OSC reinforced ground.
2. Lower S/D ratios yielded higher FOS values, lower excess pore water pressure and decreased settlement of the natural ground under the embankment. With increase in S/D ratio from 2 to 3.5, the FOS reduced from 1.25 to 1.1 and 1.75 to 1.58 for OSC- and GESC-supported embankments respectively.
3. The increase in the geosynthetic encasement stiffness improved the factor of safety considerably. With increase in the geosynthetic encasement stiffness from 500 to 4000 kN/m, the FOS values increased from 1.56 to 1.76, reduction in the excess pore water pressure and average settlement of the ground under the embankment was observed.
4. The increase in the cohesion of underlain soil improved the stability of embankments considerably. On increasing the cohesion from 5 to 40 kPa, the FOS values improved from 1.02 to 1.61, 1.11 to 1.69 and 1.64 to 1.9 for unreinforced, OSC supported and GESC-supported embankments respectively. The settlement under the embankment also reduced with increasing cohesion.
5. Increase in the friction angle of stone column resulted in improvement in the FOS values and also resulted in reduction of settlement of the ground under the embankment. Increase in friction angle of stone column infill from 30° to 42° resulted in improvement of FOS values from 1.08 to 1.13 and 1.58 to 1.67 for OSC- and GESC-supported embankments respectively and also resulted in reduced average settlement under the embankment.
6. Change in friction angle of embankment from 25° to 40° enhanced the factor of safety from 1.01 to 1.09, 1.07 to 1.18 and 1.50 to 1.87 for unreinforced, OSC supported and GESC-supported embankments respectively. The improvement is more prominent in case of GESC-supported embankments. The settlement of ground under the embankment also reduced with increasing friction angle of embankment.

7. MLR and ANN can be used as a good tool for predicting the factor of safety against the deep-seated failure.
8. The results obtained from MLR and ANN are in good agreement with the results generated from FEM analysis.
9. The correlation coefficient with FEM output when tested on an independent data set of 15 embankments for ANN (0.995) was found to be better compared with that of MLR (0.942).
10. ANN models showed lower RMSE and MAE compared with that of MLR. Hence, ANN model was able to predict the factor of safety with better accuracy.

Authors' Contributions L.A. Dar conceived this research idea, carried out the FEM, MLR and ANN analysis for embankment stability and contributed in writing the manuscript and its revision. M. Y. Shah provided guidance and participated in carrying out the FEM analysis and formulation of manuscript and its revision. Both authors have read and approved the final manuscript.

Compliance with Ethical Standards

Competing Interests The authors declare that they have no competing interests.

References

- Aboshi, H., Ichimoto, E., Enoki, M., Harada, K.: The composer—a method to improve characteristics of soft clay by inclusion of large diameter sand columns. In: Proceedings of the International Conference on Soil Reinforcement: Reinforced Earth and Other Techniques, Paris, vol. 1, pp. 211–216 (1979)
- Abusharar, S.W., Han, J.: Two-dimensional deep-seated slope stability analysis of embankments over stone column-improved soft clay. *Eng. Geol.* **120**(1), 103–110 (2011)
- Adalier, K., Elgamal, A.: Mitigation of liquefaction and associated ground deformations by stone columns. *Eng. Geol.* **72**(2004), 275–291 (2004)
- Ali, K., Shahu, J.T., Sharma, K.G.: Model tests on geosynthetic-reinforced stone columns: a comparative study. *Geosynth. Int.* **19**(4), 292–305 (2012)
- Ayadat, T., Hanna, A.M.: Encapsulated stone columns as a soil improvement technique for collapsible soil. *Ground Improv.* **9**(4), 137–147 (2005)
- Bergado, D.T., Singh, N., Sim, S.H., Panichayatum, B., Sampaco, C.L., Balasubramaniam, A.S.: Improvement of soft Bangkok clay using vertical geotextile band drains compared with granular piles. *Geotext. Geomembr.* **9**(3), 203–231 (1990)
- Briggs, K.M., Loveridge, F.A., Glendinning, S.: Failures in transport infrastructure embankments. *Eng. Geol.* **219**(2017), 107–117 (2017)
- Brokemper, D., Sobolewski, J., Alexiew, D., and Brok, C.: Design and construction of geotextile encased columns supporting geogrid reinforced landscape embankments: Bastions Vijfwal Houten in the Netherlands. *Proc., 8th Int. Conf. on Geosynthetics*, Millpress, Amsterdam, The Netherlands, 1681–1684 (2006).
- Castro, J., Cimentada, A., Costa, A., Canizal, J., Sagasetta, C.: Consolidation and deformation around stone columns: comparison of theoretical and laboratory results. *Comput. Geotech.* **49**, 326–337 (2013)
- Chakraborty, A., Goswami, D.: Prediction of slope stability using multiple linear regression (MLR) and artificial neural network (ANN). *Arab. J. Geosci.* **10**, 385 (2017)
- Cooper, M.R., Rose, A.N.: Stone column support for an embankment on deep alluvial soils. *Proceedings of the Institution of Civil Engineers, Geotechnical Engineering.* **37**(1), 15–25 (1999)
- Das, M., Dey, A.K.: Prediction of bearing capacity of stone columns placed in soft clay using ANN model. *Geotech. Geol. Eng.* (2017)
- Demuth, H., Beale, M.: *Neural network toolbox for use with MATLAB*. The Math works Inc., Natick (1995)

- Ghazavi, M., Afshar, J.N.: Bearing capacity of geosynthetic encased stone columns. *Geotext. Geomembr.* **38**, 26–36 (2013)
- Gniel, J., and Bouazza, A., 2009. "Improvement of soft soils using geogrid encased stone columns," *Geotext. Geomembr.*, vol. 27, no. 3, pp. 167–175
- Greenwood, D.A.: Mechanical Improvement of Soils below Ground Surfaces. In: Proceedings, ground engineering conference, institution of civil engineers, London, pp. 11–22 (1970)
- Han, J.: Recent advances in column technologies to improve soft soils. In: Indraratna, B., Rujikiatkamjorn, C., Vinod, J. (eds.) Invited keynote lecture, Proceedings of International Conference on Ground Improvement and Ground Control, Wollongong, Australia, 30 October to 2 November, vol. 1, pp. 99–113. Research Publishing (2012)
- Han, J., Ye, S.L.: Simplified method for consolidation rate of stone column reinforced foundation. *J. Geotech. Geoenviron. Eng. ASCE.* **127**(7), 597–603 (2001)
- Han, J., Sheth, A.R., Porbaha, A., Shen, S.L.: Numerical analysis of embankment stability over deep mixed foundations. In: *Geotechnical Engineering for Transportation Projects. Proceedings of Geo-Trans 2004*, 126 II, pp. 1385–1394. Geotechnical Special Publication, Los Angeles (2004)
- Han, J., Parsons, R.J., Sheth, A.R., Huang, J.: Factors of safety against deep-seated failure of embankments over deep mixed columns. Proceedings of Deep Mixing 2005 Conference, Sweden, vol. 1.2, pp. 231–236 (May 23–25) (2005)
- Han, J., Oztoprak, S., Parsons, R.L., Huang, J.: Numerical analysis of foundation columns to support widening of embankments. *Comput. Geotech.* **34**, 435–448 (2007)
- Hughes, J.M.O., Withers, N.J., Greenwood, D.A.: A field trial of the reinforcing effect of a stone column in soil. *Geotechnique.* **25**(1), 31–44 (1975)
- Khabbazzian, M., Meehan, C.L., Kaliakin V.N.: Column supported embankments with geosynthetic encased columns: parametric study (2014)
- Khadim, S.T., Fouad, Z.B.: Stability analysis of roadway embankments supported by stone columns with the presence of water table under short term and long term conditions. *MATECH web of conferences.* **162**, 01013 (2018)
- Kitazume, M., Maruyama, K.: External stability of group column type deep mixing improved ground under embankment loading. *Soils Found.* **46**(3), 323–340 (2006)
- Kivelo, M., Broms, B.B., 1999. Mechanical behaviour and shear resistance of lime/cement columns. International conference on dry mix methods: dry mix methods for deep soil stabilization, pp. 193–200
- Lo, S.R., Zhang, R., Mak, J.: Geosynthetic-encased stone columns in soft clay: a numerical study. *Geotext. Geomembr.* **28**(3), 292–302 (2010)
- Malarvizhi, S.N., Ilamparuthi, K., 2007. Performance of stone column encased with geogrids. Proceedings of the 4th International Conference on Soft Soil Engineering, pp. 309–314
- MATLAB (R2018a). Neural Network Toolbox- User's Guide. <https://in.mathworks.com/help/deeplearning/ref/nnstart.html>
- McKenna, J.M., Eyre, W.A., Wolstenholme, D.R.: Performance of an embankment supported by stone columns in soft ground. *Geotechnique.* **25**(1), 51–59 (1975)
- Murtaza, H.N., Samadhiya, N.K.: Experimental and numerical analysis of geosynthetic-reinforced floating granular piles in soft clays. *Int. J. of Geosynth. And Ground Eng.* **2**, 22 (2016)
- Murugesan, S., Rajagopal, K.: Geosynthetic-encased stone columns: numerical evaluation. *Geotext. Geomembr.* **24**(6), 349–358 (2006)
- Murugesan, S., Rajagopal, K.: Model tests on geosynthetic encased stone columns. *Geosynth Int J.* **24**(6), 346–354 (2007)
- Priebe, H.J.: The design of vibro replacement. *Ground Eng.* **28**(10), 31–37 (1995)
- Raithel, M., Kempfert, H.G.: Calculation models for dam foundations with geotextile-coated sand columns. In: Proceedings of the International Conference on Geotechnical and Geological Engineering (GeoEngg '00), p. 347. Australia, Melbourne (2000)
- Sharma, S.R., Phanikumar, B.R., Nagendra, G.: Compressive load response of granular piles reinforced with geogrids. *Can. Geotech. J.* **41**(1), 187–192 (2004)
- Tandel, Y.K., Solanki, C.H., Desai, A.K.: 3D FE analysis of an embankment construction on grsc and proposal of design method (2013)
- Van, I.W., Silence, P.: Improving of the bearing capacity of weak hydraulic fills by means of geotextiles. In: Proceedings of the 3rd international conference on geotextiles, Vienna, pp. 1411–1416 (1986)
- Wu, C.S., Hong, Y.S.: Laboratory tests on geosynthetic encapsulated sand columns. *Geotext. Geomembr.* **27**(2), 107–120 (2009)
- Yoo, C.: Performance of geosynthetic-encased stone columns in embankment construction: numerical investigation. *J. Geotech. Geoenviron.* **136**(8), 1148–1160 (2010)

- Yoo, C., Kim, S.B.: Numerical modeling of geosynthetic encased stone column-reinforced ground. *Geosynth. Int.* **16**(3), 116–126 (2009)
- Yoo, C., Lee, D.: Performance of geogrid-encased stone columns in soft ground: full-scale load tests. *Geosynth. Int.* **19**(6), 480–490 (2012)
- Yoo, C., Song, A., Kim, S., Lee, D.: Finite element modeling of geogrid-encased stone column in soft ground. *J. Kor. Geotech. Soc.* **23**(10), 133–150 (2007)
- Zhang, Z., Han, J., Ye, G.: Numerical investigation on factors for deepseated slope stability of stone column-supported embankments over soft clay. *Eng. Geol.* **168**, 104–113 (2014)

Publisher's Note Springer Nature remains neutral with regard to jurisdictional claims in published maps and institutional affiliations.

Affiliations

Lateef Ahmad Dar¹ · Mohammad Yousuf Shah¹

¹ Department of Civil Engineering, National Institute of Technology Srinagar, Hazratbal, Srinagar, Jammu and Kashmir 190006, India